AN ITERATIVE ALGORITHM FOR TORSION BALANCING DEEP-WATER CABLES AND UMBILICALS

Magnus Komperød*
Technological Analyses Centre
Nexans Norway AS
P. O. Box 42, 1751 HALDEN
Norway

ABSTRACT

Direct electrical heating (DEH) is a technology for preventing hydrate formation and wax deposit in oil and gas pipelines. Nexans Norway AS is currently researching and developing deep-water DEH solutions. A Nexans research project which was finished in year 2014 concludes that a deep-water DEH riser cable for 2 300 m water depth is feasible.

This paper presents an iterative algorithm for torsion balancing deep-water cables and umbilicals, using analytical considerations of the armor wires. The main advantage of this algorithm is that it does not depend on analytical expressions of the cable's torsion balance. Hence, the algorithm can be used also on cables which mechanical properties are established using finite element simulations, i.e. not only on cables where there exist analytical models of the mechanical properties.

The algorithm was initially developed for the deep-water DEH riser cable. The algorithm works very well. After two iterations the torsion unbalance was reduced by 98%.

Keywords: Cross Section Analysis; Deep-Water; DEH; Direct Electrical Heating; Offshore Technology; Subsea Cable; Torsion Balancing; Umbilical.

Notation

A_i	Cross section area of each armor wire in layer i [m^2].
E_i	E-modulus of armor wires in layer i [Pa].
EA_c	The cable's axial stiffness [N].
k	Iteration number [-].
L_i	Pitch length of armor wires in layer i [m].
l_i	Length of armor wires over one pitch length in layer i [m].
$M_i(k)$	Change of total cross section area in layer i (all armor wires) from iteration $k-1$ to iteration k [m^2].
$M_{T,c}$	The cable's torsion moment [Nm].
$M_{T,i}$	Contribution to the cable's torsion moment from each armor wire in layer i [Nm].
$N_i(k)$	Number of armor wires in layer i at iteration k [-].
$\bar{N}_i(k)$	Theoretical number of armor wires in layer i at iteration k [-].
$N_i^{\max}$	Maximum allowed number of armor wires in layer i [-].
R_i	Pitch radius of armor wires in layer i [m].
$r_i(k)$	Element radius of armor wires in layer i at iteration k [m].
$\bar{r}_i(k)$	Theoretical element radius of armor wires in layer i at iteration k [m].
T_c	Axial cable tension [N].
T_i	Axial tension of each armor wire in armor layer i [N].
α_i	Pitch angle of armor wires in layer i [rad].
$\beta_c(k)$	The cable's torsion moment to axial tension ratio at iteration k [Nm/N].
$\beta_i(k)$	Contribution to the cable's torsion moment to axial tension ratio from all armor wires in layer i at iteration k [Nm/N].

*Corresponding author: Phone: +47 69 17 35 39 E-mail: magnus.komperod@nexans.com

ε_c Axial strain of the cable [-].
ε_i Axial strain of armor wires in layer i [-].
σ_i Axial stress of armor wires in layer i [Pa].

Values with iteration number $k = 0$ refer to the initial values, i.e. the values before the torsion balancing process begins. For example $N_1(0)$ refers to the initial number of armor wires in layer 1. During general explanations where the armor layer number is not relevant, the layer number sub-script is omitted. Similarly, where the iteration number is irrelevant, the argument k is omitted.
Negative values of L indicate left lay direction, and positive values of L indicate right lay direction. Similarly, negative values of α indicate left lay direction, and positive values of α indicate right lay direction. All other length values are always positive.

INTRODUCTION

The world's increasing energy demand, combined with the exhaustion of many easily accessible oil and gas reserves, drives the petroleum industry into deeper waters. Manufacturers of subsea cables and umbilicals are among those who face the technological challenges of increased water depths.
Another significant challenge of offshore petroleum production is that the pipeline is cooled by the surrounding water. As the pipeline content drops to a certain temperature, hydrates may be formed and wax may start to deposit inside the pipeline wall. Hydrates and wax may partially, or even fully, block the pipeline. Hydrate formation may start at temperature as high as 25°C, while wax deposit may start at 35-40°C [1].
There are several ways to prevent hydrate formation and wax deposition. An intuitive solution is to apply thermal insulation at the outer surface of the pipeline. However, at long pipelines, low flow rates, or production shut downs, this solution may be insufficient.
Depressurizing the pipeline content may be used to prevent hydrate formation. However, at deep-water pipelines, high pressure is required to bring the pipeline content to topside. Plug removal by depressurizing also faces the same problem at deep-water pipelines [2].
When thermal insulation and depressurizing are insufficient, a commonly used approach is to add chemicals to the pipeline in order to reduce the critical temperature for hydrate formation and wax deposition. Methanol or glycol is commonly used [1, 3]. However, as explained in reference [1], adding chemicals has practical as well as environmental disadvantages.
Another approach to prevent hydrate formation and wax deposition is to use power cables inside the thermal insulation of the pipeline. The power cables function as heating elements heating the pipeline. However, embedding the cables inside the thermal insulation may lead to practical difficulties [1].
A technology that has emerged over the last years is direct electrical heating (DEH). The first DEH system was installed at Statoil's Åsgard oil and gas field in the Norwegian Sea in year 2000 [4]. Nexans Norway AS qualified the DEH technology together with Statoil and SINTEF.
In DEH systems, the electrical resistance of the steel in the pipeline wall is used as a heating element. A single phase cable, referred to as piggyback cable (PBC), is strapped to the pipeline. In the far end (the end of the pipeline far away from the topside) the PBC is connected ("short circuited") to the pipeline. In the near end (the end of the pipeline close to the topside), a two-phase DEH riser cable is connected to the PBC and the pipeline; one phase of the riser cable is connected to the PBC, and the other phase of the riser cable is connected to the pipeline. When the riser cable is energized topside, energy is transferred through the PBC into the steel of the pipeline wall.
Nexans Norway AS is currently developing deep-water DEH solutions. A piggyback cable that is reparable, i.e. can carry its own weight, at 1 070 m water depth is already produced by Nexans in a delivery project. When this DEH system is installed outside the coast of Africa, it will be the world's deepest DEH system [4]. A Nexans research project was finished in year 2014, which concludes that a DEH riser cable for 2 300 m is feasible. The cross section of this DEH riser cable is shown in Figure 1. Actually, already in year 2010-2011, Nexans Norway AS predicted the feasibility of such a deep-water DEH riser cable in references [5] and [6].
The deep-water DEH riser cable shown in Figure 1 has four stranded conductors (red color) with electrical insulation systems (dark gray, light gray, and black colors). Outside the conductors are two lay-

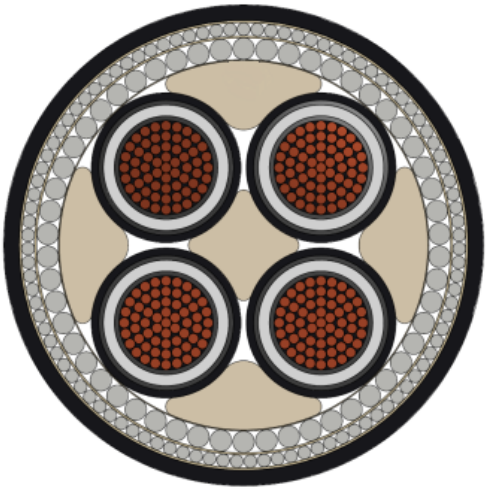

Figure 1: Cross section of the deep-water DEH riser cable, which is feasible for 2 300 m water depth.

ers of armor wires (gray color) and then the outer sheath (the outermost sheath in black color). Empty spaces are occupied with fillers (light brown color), which give better distribution of radial forces. The flexible center profile (light brown color) is patented by Nexans Norway AS. This profile in combination with the accurately developed cable geometry is essential for the cable to be installed and operated at as large water depths as 2 300 m.

For deep-water cables, the submerged weight (i.e. the net force of gravity minus buoyancy) causes large cable tension topside. For such cables, it is desirable that the cable is well torsion balanced. A poorly balanced cable will twist when being axially tensioned. If the cable is fixed in both ends, and thereby prevented from twisting, a poorly balanced cable will set up a torsion moment when being axially tensioned.

The mechanical properties of the deep-water DEH riser cable presented in Figure 1 was analyzed using a finite element method (FEM) software. Hence, there is no *analytical* expression for the cable's torsion balance that can be used for the torsion balancing process. The author then developed the iterative algorithm presented in this paper. The purpose of this algorithm is to torsion balance a cable through analytical considerations of the cable's armor wires. The main advantage of this algorithm is that it can be used even if there is only a FEM model of the cable, i.e. no analytical model. The algorithm proves to be very successful. After two iterations, the DEH riser cable's unbalance (quantified as the torsion moment to axial tension ratio) was reduced by 98%.

Analytical expressions for a cable's torsion balance are well known in the literature, see for example reference [7]. However, the author is not familiar with any algorithm which has a similar purpose as the algorithm presented in this paper, and that uses the same tuning parameters.

OBJECTIVES OF THE ALGORITHM

In subsea cables and umbilicals, steel armor is commonly used as load carrying element. There are usually two, sometimes four, layers of armor wires of alternating lay directions (left or right). The objective of the algorithm presented in this paper is to torsion balance cables and umbilicals with two armor layers of opposite lay directions. As the cable's torsion moment to axial tension ratio, β_c, is used to quantify the torsion unbalance of the cable, the mathematical formulation of the objective is to achieve $\beta_c = 0$ Nm/N.

Armor wires with circular cross sections are assumed. It is also possible to adapt the algorithm to armor wires of other cross section shapes. However, this is beyond the scope of this paper.

The tuning parameters to achieve torsion balance are the number of armor wires in each armor layer and the armor wires' radii. In other words, the tuning parameters are N_1, N_2, r_1, and r_2. Hence, the algorithm's objective is to tune these four parameters to achieve $\beta_c = 0$ Nm/N.

In Figure 1, N_2 is the number of armor wires in the outer armor layer (i.e. the armor layer right inside the black outer sheath). The parameter r_2 is the radius of each armor wire in this armor layer. Please note the difference between r_2 and R_2: r_2 is the radius of the armor wire itself, while R_2 is the distance from center of the armor wire to center of the cable. Similarly, N_1 is the number of armor wires in the inner armor layer (i.e. the armor layer right inside the outer armor layer), and r_1 is the radius of the armor wires in this layer.

In theory, there is an infinite number of combinations of the four tuning parameters that will achieve $\beta_c = 0$ Nm/N. For a solution to be feasible, two additional constraints must be introduced: (i) The cable's axial stiffness, EA_c, should not change subject to the torsion balancing. This ensures unchanged stress distribution between the armor and the other

cable elements. For realistic cable designs, this also ensures that the cable's capacity (allowed combinations of axial tension and bending curvature) will be almost unchanged. (ii) The fill factors of the armor layers (i.e. the complement of the empty space within each layer) should be unchanged.
In order to limit the complexity of the algorithm, the following simplifications are introduced: (i) Linear elastic materials are assumed. (ii) Radial displacements in the cable, including radial deformations due to the Poisson ratio effect is neglected, because radial displacements require detailed modeling of the non-armor cable elements. (iii) The armor layers' pitch radii, R_1 and R_2, are considered as constants in the algorithm, while they will be subject to small changes in real-life. As will be shown later in this paper, the algorithm gives very good results, despite these simplifications.

THE ITERATION PROCESS

The torsion balancing algorithm is an iteration process. Step 0 is performed once before the first iteration. Step 1 and step 2 are performed once for each iteration.

Step 0: The iteration counter k is set to zero, i.e. $k = 0$.

Compute or simulate the cable's axial stiffness, EA_c, and the cable's initial torsion moment to axial tension ratio, $\beta_c(0)$.

If $\beta_c(0)$ is sufficiently small (absolute value), no torsion balancing is needed.

If $\beta_c(0)$ is too large (absolute value), then go to step 1.

Step 1: Increase the iteration counter k by 1.

Calculate new values of $N_1(k)$, $N_2(k)$, $r_1(k)$, and $r_2(k)$. How to calculate these values will be explained in the next section. Then go to step 2.

Step 2: Compute or simulate the torsion moment to axial tension ratio, $\beta_c(k)$, based on $N_1(k)$, $N_2(k)$, $r_1(k)$, and $r_2(k)$ found in step 1.

If $\beta_c(k)$ is sufficiently small (absolute value), torsion balance is achieved.

If $\beta_c(k)$ is too large (absolute value), then go to step 1.

The computations of step 0 and step 2 must be based on the assumption of no cable twisting, i.e. the cable is prevented from twisting at both cable ends.
Ideally, the cable should be perfectly torsion balanced after one iteration, i.e. $\beta_c(1)$ should be zero. However, due to the simplifications introduced in the previous section, more iterations may be necessary. For the deep-water DEH riser cable presented in Figure 1, two iterations were sufficient. However, the algorithm improved the torsion balance also during the third and forth iterations.
How to compute or simulate EA_c and β_c in step 0, and β_c in step 2, is beyond the scope this paper. Analytical calculations can be used, see for example references [7] and [8]. There are also several commercial available software tools that can be used for this purpose.
The calculations of step 1 can be done using only pen, paper, and a calculator. However, a spreadsheet program or implementing a simple script will ease the work. Nexans Norway AS has implemented step 1 in a spreadsheet.

CALCULATING STEP 1

This section derives the calculations to be performed in step 1 of each iteration.

Inputs to Step 1

At iteration k, the calculation of step 1 takes the following inputs:

- $N_1(k-1)$, $N_2(k-1)$, $r_1(k-1)$, and $r_2(k-1)$. These values were computed in step 1 of iteration $k-1$ (for the first iteration the initial values are to be used). These values will be updated for each iteration.
- $\beta_c(k-1)$. This value was computed in step 2 in iteration $k-1$ (for the first iteration the value was computed in step 0). This value will be updated for each iteration.
- EA_c, E_1, E_2, R_1, R_2, α_1, and α_2. These values are fixed, i.e. they are not updated during the iteration process.

Outputs from Step 1

At iteration k, the calculations in step 1 provide the following outputs:

- $N_1(k)$, $N_2(k)$, $r_1(k)$, and $r_2(k)$. These values will be updated for each iteration. These values are to be used as inputs to step 2 of iteration k, and to step 1 of iteration $k+1$.

An Armor Wire's Contribution to the Cable's Axial Stiffness

All helical cable elements have the same helix center, which is the center of the cable's cross section. While helices are three dimensional geometries, it is common to illustrate these geometries in two dimensions as shown in Figure 2.

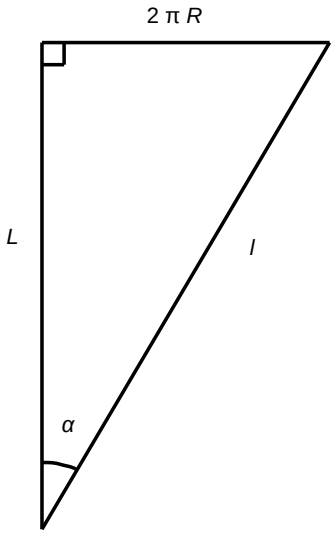

Figure 2: The geometric relationship between l, L, R, and α.

The pitch length, L, is the axial length of the cable corresponding to one revolution of the helix. Elements in the same cable layer always have the same pitch length. The element length, l, is the length of the cable element over one pitch length. The pitch radius, R, is the radius from center of the cable to center of the element. The pitch angle, α, is the angle between the cable's axis (length direction) and the tangent of the helix.

This section derives the individual wire's contribution to the cable's axial stiffness, EA_c. From Figure 2, Pythagoras' theorem gives

$$l^2 = (2\pi R)^2 + L^2. \tag{1}$$

Implicit derivation with respect to L gives

$$2l\frac{\mathrm{d}l}{\mathrm{d}L} = 2L, \tag{2}$$

$$\mathrm{d}l = \frac{L}{l}\mathrm{d}L = \cos(\alpha)\,\mathrm{d}L. \tag{3}$$

Dividing by L, and using $L = l\cos(\alpha)$, gives

$$\frac{\mathrm{d}l}{L} = \frac{\mathrm{d}l}{l\cos(\alpha)} = \cos(\alpha)\frac{\mathrm{d}L}{L}, \tag{4}$$

$$\frac{\mathrm{d}l}{l} = \cos^2(\alpha)\frac{\mathrm{d}L}{L}, \tag{5}$$

$$\varepsilon = \cos^2(\alpha)\varepsilon_c. \tag{6}$$

In Eq. 6 it is used that the cable's axial elongation is $\varepsilon_c \stackrel{\text{def}}{=} \mathrm{d}L/L$, while the element's elongation is $\varepsilon \stackrel{\text{def}}{=} \mathrm{d}l/l$. A cable element's axial tension is given as $T = EA\varepsilon$. Hence, Eq. 6 can be rewritten as

$$\varepsilon_c = \frac{\varepsilon}{\cos^2(\alpha)} = \frac{EA\varepsilon}{EA\cos^2(\alpha)} = \frac{T}{EA\cos^2(\alpha)} = \frac{T\cos(\alpha)}{EA\cos^3(\alpha)}. \tag{7}$$

Reorganizing Eq. 7 gives

$$\frac{T\cos(\alpha)}{\varepsilon_c} = EA\cos^3(\alpha). \tag{8}$$

$T\cos(\alpha)$ is the component of T along the cable's axial direction, i.e. along edge L of Figure 2. This is the component that carries part of the cable's axial tension. The cable's axial stiffness is defined as $\mathrm{EA}_c \stackrel{\text{def}}{=} T_c/\varepsilon_c$. Eq. 8 is then the contribution of an individual cable element to the cable's axial stiffness, EA_c. Hence, the contribution to EA_c from all armor wires in armor layer i is

$$N_i E_i A_i \cos^3(\alpha_i). \tag{9}$$

An Armor Wire's Contribution to the Cable's Torsion Balance

This section derives the individual armor wire's contribution to the cable's torsion moment to axial tension ratio. The axial tension of a cable element, T, acts along edge l of Figure 2. The component $T\sin(\alpha)$, i.e. along the edge $2\pi R$ in the figure, acts in the circumferential direction of the cable, i.e normal to the cable's length direction and normal to the

cable's radius. This force component sets up a torsion moment, which lever arm is the cable element's pitch radius, R. Hence, the torsion moment caused by an individual armor wire, M_T, is the lever arm, R, multiplied by the force component, $T\sin(\alpha)$, i.e.

$$\begin{aligned} M_T &= RT\sin(\alpha) = EAR\varepsilon\sin(\alpha) \\ &= EAR\varepsilon_c\cos^2(\alpha)\sin(\alpha). \end{aligned} \tag{10}$$

In Eq. 10 it is used that $T = EA\varepsilon$, and Eq. 6 is inserted. Inserting the definition of the cable's axial stiffness into Eq. 10 gives

$$M_T = EAR\cos^2(\alpha)\sin(\alpha)\frac{T_c}{\mathrm{EA}_c}, \tag{11}$$

$$\beta \stackrel{\text{def}}{=} \frac{M_T}{T_c} = \frac{EAR\cos^2(\alpha)\sin(\alpha)}{\mathrm{EA}_c}. \tag{12}$$

In Eq. 12, β is the cable element's contribution to the cable's torsion moment to axial tension ratio, β_c. Hence, the contribution to β_c from all armor wires in armor layer i is

$$\beta_i = \frac{N_i E_i A_i R_i \cos^2(\alpha_i)\sin(\alpha_i)}{\mathrm{EA}_c}. \tag{13}$$

Calculating the Number of Armor Wires and the Wire Radii

Eq. 9 expresses an armor layer's contribution to the cable's axial stiffness, EA_c. Hence, for EA_c to be constant from iteration $k-1$ to k, it must be required that

$$\begin{aligned} &N_1(k)E_1A_1(k)\cos^3(\alpha_1) \\ &+N_2(k)E_2A_2(k)\cos^3(\alpha_2) \\ =&N_1(k-1)E_1A_1(k-1)\cos^3(\alpha_1) \\ &+N_2(k-1)E_2A_2(k-1)\cos^3(\alpha_2). \end{aligned} \tag{14}$$

Eq. 14 can be rewritten to

$$M_1(k)E_1\cos^3(\alpha_1) + M_2(k)E_2\cos^3(\alpha_2) = 0, \tag{15}$$

where

$$M_i(k) \stackrel{\text{def}}{=} N_i(k)A_i(k) - N_i(k-1)A_i(k-1). \tag{16}$$

From Eq. 13 the change of armor layer i's contribution to β_c from iteration $k-1$ to k is

$$\begin{aligned} &\beta_i(k) - \beta_i(k-1) \\ &= [N_i(k)A_i(k) - N_i(k-1)A_i(k-1)] \\ &\quad\times \frac{E_iR_i\cos^2(\alpha_i)\sin(\alpha_i)}{\mathrm{EA}_c} \\ &= \frac{M_i(k)E_iR_i\cos^2(\alpha_i)\sin(\alpha_i)}{\mathrm{EA}_c}. \end{aligned} \tag{17}$$

The change of β_c from $k-1$ to k is

$$\begin{aligned} &\beta_c(k) - \beta_c(k-1) \\ &= [\beta_1(k) - \beta_1(k-1)] + [\beta_2(k) - \beta_2(k-1)]. \end{aligned} \tag{18}$$

The objective of the algorithm is to achieve $\beta_c = 0$. Inserting Eq. 17 and $\beta_c(k) = 0$ into Eq. 18 gives

$$\begin{aligned} -\beta_c(k-1) =& \frac{M_1(k)E_1R_1\cos^2(\alpha_1)\sin(\alpha_1)}{\mathrm{EA}_c} \\ &+ \frac{M_2(k)E_2R_2\cos^2(\alpha_2)\sin(\alpha_2)}{\mathrm{EA}_c}. \end{aligned} \tag{19}$$

Eq. 15 and Eq. 19 make a set of equations which is linear in $M_1(k)$ and $M_2(k)$. Solving with respect to $M_1(k)$ and $M_2(k)$ gives

$$\begin{aligned} &M_1(k) \\ &= \frac{-\beta_c(k-1)\mathrm{EA}_c\cos(\alpha_2)}{E_1\left[R_1\cos^2(\alpha_1)\sin(\alpha_1)\cos(\alpha_2) - R_2\cos^3(\alpha_1)\sin(\alpha_2)\right]}, \end{aligned} \tag{20}$$

$$\begin{aligned} &M_2(k) \\ &= \frac{-\beta_c(k-1)\mathrm{EA}_c\cos(\alpha_1)}{E_2\left[R_2\cos(\alpha_1)\cos^2(\alpha_2)\sin(\alpha_2) - R_1\sin(\alpha_1)\cos^3(\alpha_2)\right]}. \end{aligned} \tag{21}$$

Eq. 20 and Eq. 21 express how much the total cross section area of all armor wires in armor layer 1 and 2, respectively, must be changed for the cable to be torsion balanced, while preserving its axial stiffness. However, the equations contain insufficient information to decide $N_i(k)$ and $r_i(k)$. This will be addressed next.

In the derivation to follow, the notation $\bar{N}_i(k)$ and $\bar{r}_i(k)$ will be used instead of $N_i(k)$ and $r_i(k)$, respectively. $\bar{N}_i(k)$ and $\bar{r}_i(k)$ are temporarily theoretical

values that are not constrained to $\bar{N}_i(k)$ being an integer.

Under the assumption of constant pitch radii for both armor layers, the requirement of constant fill factors can be expressed as

$$\bar{N}_i(k)\bar{r}_i(k) = N_i(k-1)r_i(k-1). \quad (22)$$

Using $A_i = \pi {r_i}^2$, Eq. 16 can be rewritten to

$$\pi\bar{N}_i(k)\bar{r}_i(k)^2 = \pi N_i(k-1)r_i(k-1)^2 + M_i(k). \quad (23)$$

Inserting Eq. 22 into Eq. 23 and solving for $\bar{r}_i(k)$ gives

$$\bar{r}_i(k) = r_i(k-1) + \frac{M_i(k)}{\pi N_i(k-1)r_i(k-1)}. \quad (24)$$

Then inserting Eq. 24 into Eq. 22 and solving for $\bar{N}_i(k)$ obtains

$$\bar{N}_i(k) = \frac{\pi N_i(k-1)^2 r_i(k-1)^2}{\pi N_i(k-1)r_i(k-1)^2 + M_i(k)}. \quad (25)$$

Eq. 24 and Eq. 25 give values for $\bar{N}_i$ and $\bar{r}_i$ that torsion balance the cable, while preserving the cable's axial stiffness and the layers' fill factors. However, these values are infeasible because $\bar{N}_i$ is not constrained to being an integer. Now the notation N_i and r_i are re-introduced, where N_i is an integer. The true number of armor wires in layer i can be computed as

$$\begin{aligned} &N_i(k) \quad (26)\\ &= \min\left(\lfloor \bar{N}_i(k) \rfloor, N_i^{\max}\right)\\ &= \min\left(\left\lfloor \frac{\pi N_i(k-1)^2 r_i(k-1)^2}{\pi N_i(k-1)r_i(k-1)^2 + M_i(k)} \right\rfloor, N_i^{\max}\right). \end{aligned}$$

In Eq. 26, $\min(\cdot)$ is the function that returns the lowest of its arguments. The floor function, $\lfloor \cdot \rfloor$, truncates downward to the nearest integer. Using the floor function, instead of the ceil function, ensures that the fill factors do not increase, which could have resulted in over-filled armor layers. $N_i^{\max}$ is an upper limit of the number of armor wires, which is set based on practical considerations.

Replacing $\bar{N}_i(k)$ and $\bar{r}_i(k)$ with $N_i(k)$ and $r_i(k)$, respectively, in Eq. 23, and solving for $r_i(k)$ gives the true radii of the armor wires in each layer

$$r_i(k) = \sqrt{\frac{\pi N_i(k-1)r_i(k-1)^2 + M_i(k)}{\pi N_i(k)}}. \quad (27)$$

The calculations to be performed in step 1 of the torsion balancing algorithm can then be summarized as

1. Calculate $M_1(k)$ and $M_2(k)$ from Eq. 20 and Eq. 21, respectively.
2. Calculate $N_1(k)$ and $N_2(k)$ from Eq. 26.
3. Calculate $r_1(k)$ and $r_2(k)$ from Eq. 27.

$M_i(k)$ is a temporary variable that is used for calculating $N_i(k)$ and $r_i(k)$. When $N_i(k)$ and $r_i(k)$ have been calculated, $M_i(k)$ is abandoned.

Eq. 22 ensures constant fill factor only if R_i is constant, which is an approximation. If the true R_i is decreased for one or both armor layers, it is recommended to verify that the fill factor has not become too high. If the fill factor is too high, it can be reduced by setting $N_i^{\max}$ in Eq. 26 to a value lower than $N_i(k)$, and then re-calculate $N_i(k)$ and $r_i(k)$.

TORSION BALANCING THE DEEP-WATER DEH RISER

The torsion balancing algorithm presented in this paper was initially developed for the deep-water DEH riser cable shown in Figure 1.

Initially, the torsion moment to axial tension ratio, β_c, was 1.2×10^{-3} Nm/N. After two iterations of torsion balancing, β_c is reduced by 98% to 2.2×10^{-5} Nm/N. After four iterations, β_c is reduced by more than 99.9% to 8.6×10^{-7} Nm/N.

Although the torsion balance improves significantly over the third and forth iteration, it is believed that this is only of academic interest. In practice, due to tolerances of the armor wires as well as during production of the cable, it seems unlikely that the improvements over the third and forth iterations will be present in the real-life cable.

Figure 3 illustrates how the cable's torsion moment to axial tension ratio, β_c, improves over each iteration of the torsion balancing algorithm. Note that the scale of the figure is logarithmic.

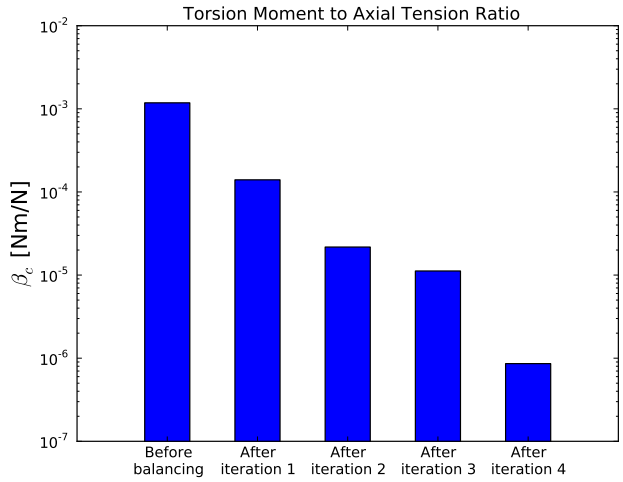

Figure 3: Improvement of β_c for each iteration. Note that the scale is logarithmic.

CONCLUSIONS

This paper derives an iterative algorithm for torsion balancing deep-water cables and umbilicals. The algorithm was developed during a research project where Nexans Norway AS concluded that a deep-water DEH riser cable for 2 300 m water depth is feasible.

The torsion balancing algorithm works very well. After two iterations, the torsion unbalance of the deep-water DEH riser cable (quantified as the cable's torsion moment to axial tension ratio) is reduced by 98%.

REFERENCES

[1] A. Nysveen, H. Kulbotten, J. K. Lervik, A. H. Børnes, M. Høyer-Hansen, and J. J. Bremnes. Direct Electrical Heating of Subsea Pipelines - Technology Development and Operating Experience. *IEEE Transactions on Industry Applications*, 43:118 – 129, 2007.

[2] J. K. Lervik, M. Høyer-Hansen, Ø. Iversen, and S. Nilsson. New Developments of Direct Electrical Heating for Flow Assurance. In *Proceedings of the Twenty-second (2012) International Offshore and Polar Engineering Conference - Rhodes, Greece*, 2012.

[3] S. Dretvik and A. H. Børnes. Direct Heated Flowlines in the Åsgard Field. In *Proceedings of the Eleventh (2001) International Offshore and Polar Engineering Conference - Stavanger, Norway*, 2001.

[4] S. Kvande. Direct Electrical Heating Goes Deeper. *E&P Magazine June 2014*, 2014.

[5] R. Slora, S. Karlsen, S. Lund, P. A. Osborg, and K. Heide. Qualification of Dynamic Deep Water Power Cable. In *Proceedings of the 2010 Offshore Technology Conference - Houston, Texas, USA*, 2010.

[6] R. Slora, S. Karlsen, and P. A. Osborg. Mechanical Qualification of Dynamic Deep Water Power Cable. In *Proceedings of the 30th International Conference on Ocean, Offshore and Arctic Engineering, OMAE 2011 - Rotterdam, the Netherlands*, 2011.

[7] R. H. Knapp. Derivation of a new stiffness matrix for helically armoured cables considering tension and torsion. *International Journal for Numerical Methods in Engineering*, 14:515 – 529, 1979.

[8] E. Kebadze. *Theoretical Modelling of Unbonded Flexible Pipe Cross-Sections*. PhD thesis, South Bank University, 2000.